LONDON2007

P176

Seismic Imaging Using Lateral Adaptive Windows

O. Pedersen* (Norwegian University of Science & Technology), S. Brandsberg-Dahl (BP America) & B. Ursin (Norwegian University of Science & Technology)

SUMMARY

We present a migration method using one-way propagators and lateral adaptive windows for handling the large velocity contrasts associated with salt-sediment interfaces. Using the adaptive windowing, we can handle the large perturbations locally in a similar fashion as the Beamlet propagator, hence limiting the impact of the errors on the global wavefield. We illustrate the performance of our method by applying it to synthetic data from the SEG/EAGE salt model.

Introduction

Accurate imaging of seismic data in areas with strong velocity contrast is becoming increasingly important as the search for hydrocarbons enters areas with very complex geology. Currently there is a large interest in salt provinces, for example the Gulf of Mexico and the West coast of Africa. When salt is present, the migration algorithm must be able to handle large velocity contrasts since the velocity in salt is generally much higher than in the surrounding sediments. The salt bodies will act as sonic lenses, dissipating or concentrating energy in a "random way" (O'Brien and Gray, 1996). Proper handling of these focusing effects in the migration algorithm is crucial for getting a proper migrated image of the sub-salt structures.

A variety of migration methods are used in sub-salt imaging, and normally we classify them as either Kirchhoff or wavefield extrapolation migrations depending on the underlying assumptions (Bleistein, 1987; Gazdag, 1978; Stolt, 1978). Kirchhoff methods implicitly impose a high frequency assumption on the wave equation and typically use ray-tracing based methods to model the wave propagation in the subsurface. Most wavefield methods are based on one-way extrapolation of the wavefield. The one-way operators are both computationally cheap and robust. Different implementations can handle varying degrees of lateral velocity variations, but in general the cost of these methods goes up as a function of medium complexity. All one-way methods will split the velocity model into a set of depth slabs and then apply the wavefield extrapolator to the wavefield, stepping it down into the model, one depth step at a time. Ferguson and Margrave (2005) introduced the notion of planned seismic imaging, where they in each depth slab select a propagator that is optimal from a performance point of view.

Here, we build on these ideas and present an extrapolation operator that in lateral windows within a slab uses an optimal local extrapolator. The scheme is especially targeted for sub-salt imaging where we have to handle the large velocity contrasts associated with the salt-sediment interfaces. For each slab of the velocity model, we will first identify the "interesting" areas in the medium, i.e. we find the areas with high lateral medium perturbations. Next, we perform an adaptive windowing construction by separating the model into sediments, salt and the salt boundary. Finally, we choose an appropriate extrapolation operator for each window. We will introduce a partition of unity to do the operator composition. The resulting operator handles the large lateral velocity perturbations locally, hence like the Beamlet method (Chen et al., 2006), it limits the spatial influence of any errors this introduces in the global wavefield. We demonstrate the accuracy of the method with application to some industry standard synthetic data sets.

One-way wavefield extrapolation

When the lateral velocity contrast is small (smooth), the split-step (SS) operator (Stoffa et al., 1990) is both cheap and accurate. The Generalized Screen (GS) operator (Wu and Huang, 1992) can handle larger velocity contrasts, but is computationally more expensive. Both the SS and GS methods are based on the thin-slab approximation, where the velocity in each thin slab is separated into a background and a perturbation part. Recently, the Beamlet propagator (Chen et al., 2006) has been introduced. Differently from the above methods, this operator uses a local reference velocity and can in principle handle media with very strong lateral velocity variations. In the Beamlet method, the velocity model for each slab is divided into lateral regular windows, where the local (windowed) velocity is again analyzed and separated into a background and a perturbation part. This will in most situations yield a more accurate operator since the local perturbations will be smaller except for in windows that contain a salt boundary. The Beamlet propagator is more expensive than both the SS and GS methods.

For simplicity in the further developments, we will only consider an isotropic $2D$ medium. An extension to $3D$ medium is straight forward following the same logic as for the Beamlet operator (Chen et al., 2006). Let Ψ denote the wave-field, z the preferred direction of propagation, and x the transverse

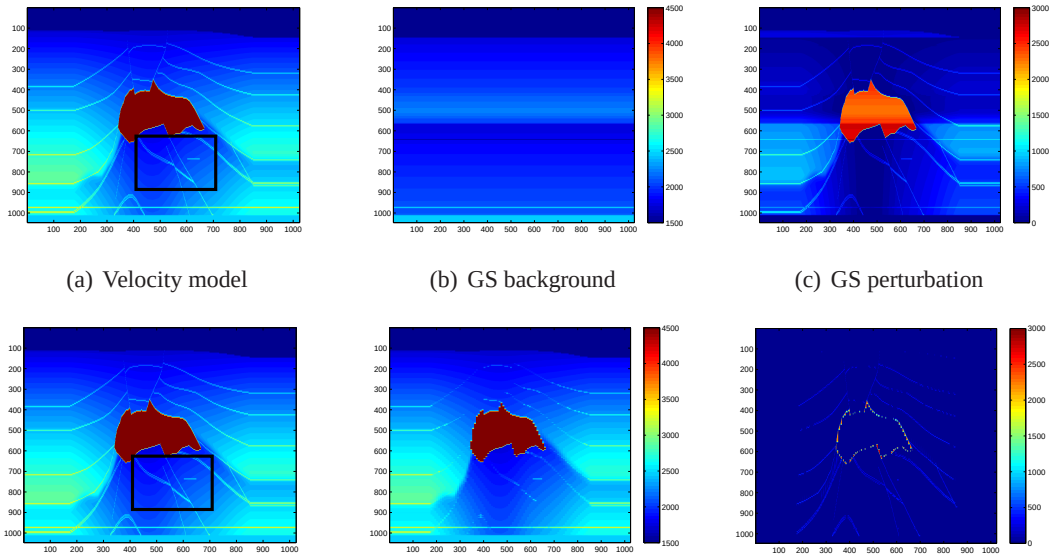

(a) Velocity model (b) GS background (c) GS perturbation

(d) Velocity model (e) Beamlet background (f) Beamlet perturbation

Figure 1: Illustration of how the background velocities and perturbations are for the GS (top) and the Beamlet method (bottom).

direction. Then the scalar wave equation is given by

$$\nabla^2 \Psi(x,z,\omega) = (\mathrm{i}k(x,z,\omega))^2 \Psi(x,z,\omega), \tag{1}$$

where $k(x,z,\omega) = \omega/v(x,z)$ is the wave number, v is the scalar wave speed (velocity), and ω is the temporal frequency. With the thin-slab approximation, i.e. $\partial_z v(x,z) = 0$ within each slab of thickness Δz, and by assuming $\partial_x v(x,z)$ is small, the wave-field $\Psi(x, z+\Delta z, \omega)$ can for each frequency be approximated by

$$\Psi(x, z+\Delta z) = \frac{1}{(2\pi)^2} \int \alpha(x, k_x, \Delta z) \stackrel{\wedge}{\Psi}(k_x, z) \mathrm{e}^{-\mathrm{i}k_x x} \mathrm{d}k_x \ , \tag{2}$$

where the symbol α is given by $\alpha(x, k_x, \Delta z) = \mathrm{e}^{\mathrm{i}\Delta z k_z(x,k_x)}$, and $\wedge$ indicates a quantity in the Fourier domain. We implement the one-way migration algorithm by slicing the velocity model into thin slabs in the preferred direction of propagation z. Within each slab, the velocity $v(x,z)$ is separated into a background part $v_0(z)$, and a perturbation part $\delta v(x,z)$ such that $v(x,z) = v_0(z) + \delta v(x,z)$. For the SS and GS methods, the background medium $v_0(z)$ is assumed to be constant within each thin slab of thickness Δz. v_0 is chosen such that $v_0(z) = \min_x v(x,z)$, since we can only perturb in one direction. In Figure 1 we see the decomposition of the velocity model for the GS and Beamlet method for the EAGE/SEG salt model. From the figures we see that for the GS method (Figure 1 (c)), the medium-perturbations are large in and around the salt body, while the medium perturbations for the Beamlet method shown in Figure 1 (f) are large only in the windows that contain the salt boundary.

In our new windowed extrapolator, we will adapt the method described above, but we will do so for individual lateral windows. In a typical slab, we will have three kinds of windows: windows that only contain sediments, windows that contain a salt-sediment interface and windows that only contain salt. In a standard salt-sediment geology, the only windows with any challenging velocity contrast will be those that contain the boundary. Hence, we can apply a cheap operator, like SS, in all windows except for those with a boundary. The more expensive and accurate operator only have to be applied in windows that contain a salt-sediment interface. More formally, for each depth level z in the model, we find a collection of boundary points $\{x_j\}$, where x_j denotes the lateral samples where we go from sediments to salt, or vice versa. We choose $\{\phi_j\}, \{\psi_j\}$ as

$$\begin{aligned} \phi_j(x) &= \chi_C^S[x_{j-1} + c : x_j - c], \\ \psi_j(x) &= \chi_C^S[x_{j-1} - c - K : x_j + c + K], \end{aligned} \tag{3}$$

such that $\sum_j(\phi_j + \psi_j)(x) = 1$ for all x. χ_C^S is an appropriate window-function. The coefficient c denotes the half number of samples on the window that is not tapered, while the coefficient K denotes the half number of samples on the tapered part of the window, as shown in Figure 2

After identifying all salt-sediment interfaces within a thin slab, the total wave-field in this slab Ψ can be represented as the superposition of its windowed components,

$$\Psi(x,z,\omega) = \sum_{i\in\mathbb{Z}} \phi_j(x)\Psi(x,z,\omega) = \sum_{i\in\mathbb{Z}} \Psi_j(x,z,\omega), \tag{4}$$

where $\{\phi_j : j \in \mathbb{Z}\}$ is the partition of unity. For each window j we assign a suitable extrapolation

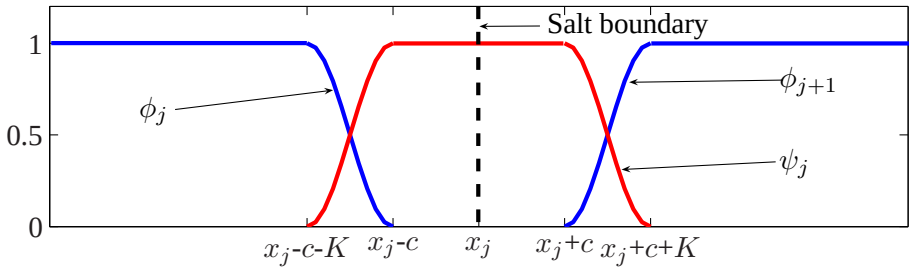

Figure 2: Adaptive windowing function.

operator P_j, thus the wave-field on the next depth is given by

$$\Psi(x,z+\Delta,\omega) = \sum_j P_j(\Psi_j(x,z,\omega)), \tag{5}$$

where Ψ_j is defined in Equation 4. We choose P in a "planned" fashion according to the local velocity contrast in the window. For windows with small contrast, we can use a simple operator like the SS, while we need the GS or Beamlet operator in the windows containing the salt interface.

Example

To illustrate the effects of the adaptive lateral windowing, we use the same model as in Figure 1. Figure 3 shows the decomposition of the velocity model for the adaptive lateral windowing scheme

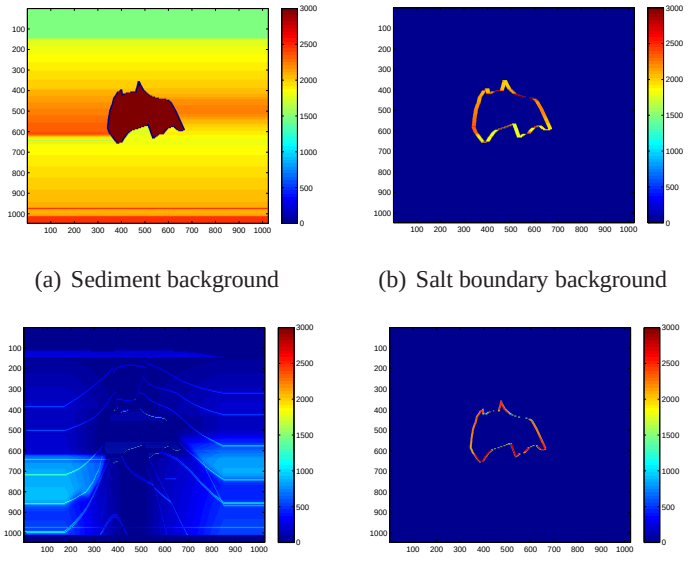

(a) Sediment background (b) Salt boundary background

(c) Sediment perturbation (d) Salt boundary perturbation

Figure 3: Background velocities (top) and velocity perturbations (bottom).

described above. Figures 3 (a) and (c) shows v_0 and δv for the sediments and salt respectively, and

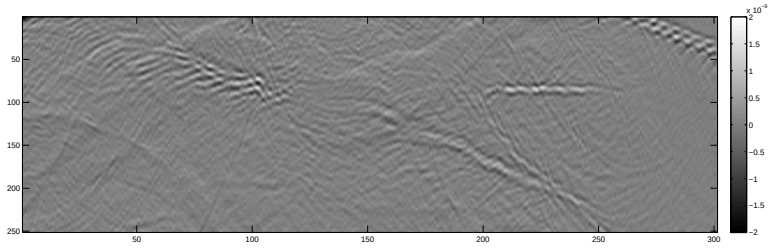

(a) Split-step propagator

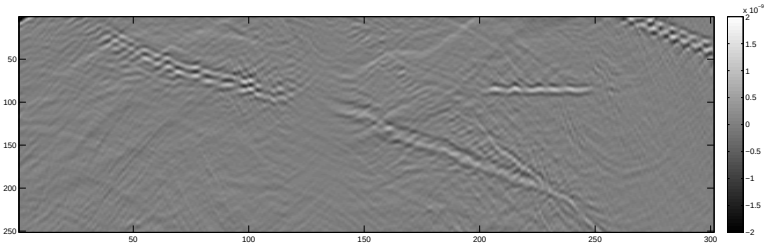

(b) Windowed split-step propagator

Figure 4: Subsalt reflector with and without adaptive lateral windowing.

Figures 3 (b) and (d) show v_0 and δv for the salt boundary. The decomposition use 1-11 windows, compared to the Beamlet method which used 128 windows. We generated synthetic data using a finite-difference modeling program and migrated the data using both the split-step method and the new adaptive lateral window method. We have used $c = K = 4$ in equation 4, and P_j is the split-step operator for all j. In Figure 4, we compare the methods on a reflector beneath the salt dome, indicated by the black box in Figure 1. The image of the dipping reflector is improved in the sub-salt region due to the improved treatment of the lateral velocity contrast in the model.

Conclusions

We have developed a new method for subsalt imaging based on one-way extrapolation operators and laterally adaptive windows. By using lateral windows we can apply a computationally cheap operator in most of the thin slab except for in the windows that contain a salt-sediment interface. We show that the new method, even when using a split-step operator in all windows, improve the image quality subsalt in our synthetic test case.

Acknowledgments

This research was developed during a BP internship in 2006. We would like to thank BP for allowing us to publish this work.

References

Bleistein, N. [1987] On the imaging of reflectors in the earth. Geophysics, 52, 931–942.

Chen, L., Wu, R.-S., and Chen, Y. [2006] Target-oriented beamlet migration based on gabor-daubechies frame decomposition. Geophysics, 71, S37–S52.

Ferguson, R. J., and Margrave, G. F. [2005] Planned seismic imaging using explicit one-way operators. Geophysics, 70, S101–S109.

Gazdag, J. [1978] Wave equation migration with the phase-shift method. Geophysics, 43, 1342–1351.

O'Brien, M. J., and Gray, S. H. [1996] Can we image beneath salt? The Leading Edge, 15(1), 17–22.

Stoffa, P. L., Fokkema, J. T., de Luna Freire, R. M., and Kessinger, W. P. [1990] Split-step fourier migration. Geophysics, 55, 410–421.

Stolt, R. H. [1978] Migration by fourier transform: Geophysics, 43, 23–48.

Wu, R.-S., and Huang, L.-J. [1992] Scattered field calculation in heterogeneous media using a phase-screen propagator. SEG Technical Program Expanded Abstracts, 11, 1289–1292.